

Bistability of thermal donors in germanium: Assignment of far-infrared and electron-paramagnetic-resonance spectra

P. Clauws, F. Callens, F. Maes, J. Vennik, and E. Boesman

Laboratorium voor Kristallografie en Studie van de Vaste Stof, Rijksuniversiteit Gent, Krijgslaan 281-S1, B-9000, Gent, Belgium

(Received 2 January 1991; revised manuscript received 4 April 1991)

Bistability of different thermal donor (TD) species in oxygen-doped germanium has been observed in far-infrared and EPR spectra. The phenomenon has been used to establish the correspondence of the spectra found in the two experiments, resulting in the identification of the EPR spectrum of the species TD2 to TD5. The spectra reveal C_{2v} symmetry for TD2 and TD5 and C_{3v} symmetry for TD3 and TD4. The results are explained in terms of neutral double donors with $S=1$. In addition, the spectrum of singly ionized TD species has been observed with use of compensated samples. The spectrum, which is assigned to a superposition of TD3 and TD4, reveals trigonal symmetry and the data can be fitted assuming $S=\frac{1}{2}$.

I. INTRODUCTION

Heat treatment of oxygen-doped germanium in the temperature range 300–450°C generates thermal donors (TD's), which are in many respects similar to the well-known TD's in silicon. In both semiconductors the TD's have been identified as a hierarchy of heliumlike double donors with only slightly different ground-state energies; the different members in the hierarchy can be resolved by infrared (IR) absorption spectroscopy. In germanium the ladder of observed TD ground states ranges from 14.3 to 18.1 meV below E_C for the neutral charge state TD⁰ and from 31.0 to 40.5 meV below E_C for the singly ionized charge state TD⁺; the corresponding series in the far-IR spectrum have been labeled *A* to *I*, etc., in order of decreasing binding energy.^{1–3}

For the past few years it has been known that the early TD species in germanium display bistable properties similarly to TD's in silicon. It was found by the Hall effect^{4,5} and by far-IR and deep-level transient spectroscopy (DLTS) experiments⁶ that the defects may occur in two configurations: the first configuration, which is metastable, gives rise to the familiar shallow double donor states; the second configuration forms a negative *U* system with a deep neutral state. TD members that show bistable behavior in a particular sample (a property that depends on the Fermi-level position), can be made to show up in the far-IR spectrum or to disappear, by an appropriate choice of cooling or heating conditions. The detailed investigation of the phenomenon by Clauws and Vennik^{6,7} made it possible to unravel the overlapping spectral series belonging to different TD members and to correlate TD members observed in IR with individual TD members characterized electrically,^{4,5} resulting in the assignment of the spectrum of the TD members TD1 to TD5.

In a recent paper, Callens *et al.*⁸ reported the discovery in oxygen-doped germanium of an EPR spectrum with C_{2v} symmetry (called there spectrum 1), which was attributed to neutral shallow TD's with $S=1$. Other

spectra (spectra 2 and 3) with trigonal symmetry were also observed, but their correlation with TD's was less certain. More recently, Bekman *et al.*⁹ succeeded in correlating the EPR spectrum 1 with the far-IR series *F*, making use of the 100% bistability of that particular donor, as revealed in a far-IR witness sample. Bekman *et al.* also presented a spin Hamiltonian, which allowed them to reproduce the splitting of the C_{2v} pattern of spectrum 1. The observation of a bistable TD in EPR, together with the high anisotropy of the *g* tensor in germanium, opened favorable perspectives for assigning separate EPR spectra to individual TD members.

In the present paper we report the observation of four different paramagnetic centers in germanium samples with high TD concentration. The percentage bistability displayed by each of the spectra will be used as a helpful tool for the mutual distinction and for the correlation with TD members identified in far-IR witness samples. In addition to the EPR spectra belonging to the neutral charge state, an EPR spectrum of singly ionized TD's in compensated germanium will be presented.

II. EXPERIMENT

The samples were selected from two kinds of oxygen-doped germanium crystals, with an interstitial oxygen concentration $[O_i]=5\times 10^{16}$ and 2×10^{17} atoms/cm³, respectively. Samples were measured as grown or were annealed at 350°C for TD formation; before the anneal a 5-min pretreatment at 900°C followed by a room-temperature quench was given (oxygen dispersion). In similar "oxygen-only" samples the free-electron density of $n=10^{14}$ to 10^{16} cm⁻³ is mainly determined by the thermal donor concentration, the shallow dopants (phosphorus) amounting to only a few times 10^{12} atoms/cm³. Compensated samples were prepared by diffusion of copper from an evaporated layer; the diffusion took place at 650°C during 1 h and was followed by a room-temperature quench and a TD-formation anneal.

Samples for EPR experiments had typical dimensions

of $10 \times 1.5 \times 1.5 \text{ mm}^3$ with the largest dimension in a $\langle 110 \rangle$ direction, for rotation of the magnetic field in the corresponding (110) plane. In one case the longest dimension was approximately along a $\langle 111 \rangle$ direction.

The far-IR spectra were recorded using a Fourier-transform spectrometer equipped with a liquid-He-cooled Ge:Ga bolometer. Band-gap light to illuminate the sample during cooling or measurement was provided by a tungsten source and a monochromator set at $1.6\text{-}\mu\text{m}$ wavelength.

The EPR spectra were recorded using a Bruker ESP300 X-band spectrometer, equipped with an Oxford ESR-10 flow cryostat. The magnetic field was modulated at 100 kHz with a peak-to-peak amplitude of 10^{-4} T . All spectra were normalized to 9.47 GHz. The best detection conditions for the spectra discussed below were low temperature ($T \approx 2 \text{ K}$) and high microwave power (20 mW).

III. NEUTRAL THERMAL DONORS

A. Far-IR results

In this section a summary is given of the far-IR investigations of bistable thermal donors in germanium, to which the EPR results will be compared; more details may be found in the papers by Clauws and Vennik.^{6,7} The lines are designated in agreement with the labels introduced in Refs. 3 and 6.

The 100% bistability of a thermal donor is detected as follows: when the sample has been slowly cooled in the dark from room temperature to the measurement temperature of $T \approx 8 \text{ K}$ the series is absent from the spectrum, while after slowly cooling under illumination with band-gap light the series is present; an alternative to illumination is quenching to low temperature, which yields comparable results. The additional absorption is metastable; it disappears when the sample temperature has been raised to 180–200 K.

Figure 1 summarizes the three cases of bistability that up to now have been investigated with far-IR spectroscopy, using samples with different TD content. The spectral range reproduced has been restricted to the $1s \rightarrow 2p_0$ transitions, which is the most useful range for the present purpose (the lines in this range are well separated from the complicated range of the $1s \rightarrow np_{\pm}$ lines, which suffers from spectral congestion, concentration broadening, and excessive absorption in samples with high TD density). The line positions relevant to the present paper are summarized in Table I.

Figure 1(a) represents the case of 100% bistability of (D, E, F'), which are the "earliest" series (i.e., corresponding with the deepest ground states) observed in samples with low TD density. The series F, G, H remain unchanged (see Ref. 6 for a detailed discussion of this case).

In Fig. 1(b) the TD concentration is higher, resulting in stronger absorption. The series D, E, F' are no longer present; on the other hand, new absorption (I) begins to appear at the lower wave-number side. It is now the series F that displays 100% bistability, while the series with shallower ground state remain unchanged. Figure

1, spectrum (b), represents the far-IR reference that was used by Bekman *et al.*⁹ to correlate the bistable EPR spectrum 1 with the far-IR series F .

Figure 1(c) shows the spectra of a sample with the highest TD concentration investigated up to now; it is of

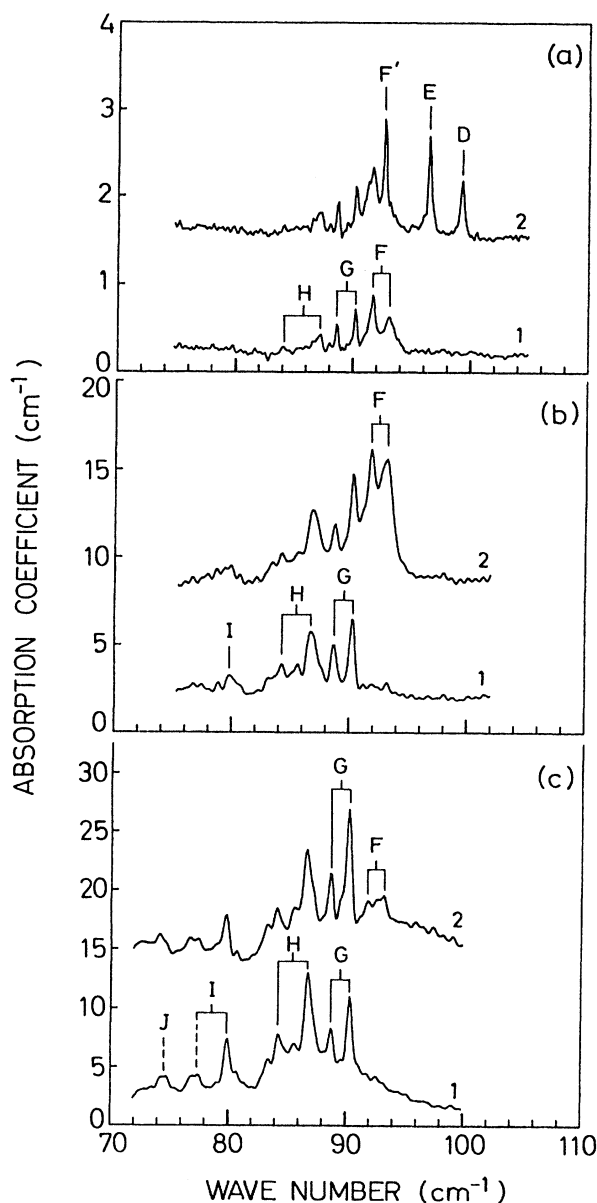


FIG. 1. Observation of bistable behavior in the far-IR absorption spectrum of neutral thermal donors in germanium; $1s \rightarrow 2p_0$ transitions; measurement temperature, $T \approx 7 \text{ K}$; the line positions are given in Table I. (a) $[\text{O}_i] = 5 \times 10^{16} \text{ atoms/cm}^3$; as-grown sample; $n(300 \text{ K}) = 2 \times 10^{14} \text{ cm}^{-3}$; (1) slowly cooled in the dark; (2) cooled with band-gap light on. (b) $[\text{O}_i] = 2 \times 10^{17} \text{ atoms/cm}^3$; oxygen dispersion at 900°C followed by TD formation at 350°C , 22 min; $n(300 \text{ K}) = 3 \times 10^{15} \text{ cm}^{-3}$; (1) slowly cooled in the dark; (2) cooled with band-gap light on. (c) $[\text{O}_i] = 2 \times 10^{17} \text{ atoms/cm}^3$; as-grown sample; $n(300 \text{ K}) = 1 \times 10^{16} \text{ cm}^{-3}$; (1) slowly cooled in the dark; (2) quenched to 77 K within a few seconds.

TABLE I. Identification of far-IR thermal donor series in germanium by the position of $1s \rightarrow 2p_0$ lines.

Series	<i>D</i>	<i>E</i>	<i>F'</i>	<i>F</i>	<i>G</i>	<i>H</i>	<i>I</i>	<i>J</i>
$1s \rightarrow 2p_0$ (cm^{-1})	99.2	96.5	92.7	93.1 91.7	90.2 88.7	87.2 86.8 84.3	80.0 77	74

this kind of sample that EPR results are reported in Sec. III B. In order to ensure a perfect mutual correspondence of spectra, the metastable configuration was produced in identical circumstances as those for the EPR experiments, i.e., by quenching instead of illumination. In Fig. 1(c) the spectrum is dominated by strong contributions of *G*, *H*, and *I*. A small contribution of *F* displays 100% bistability. The lines *G* also depend on the cooling rate: an increase of about 40% is obtained by quenching. The lines of *H*, *I*, and *J* remain unchanged.

Litvinov, Palchik, and Urenev^{4,5} have analyzed their differential Hall-effect data of oxygen-doped germanium in terms of the bistability of the three “earliest” thermal donor species TD1, TD2, and TD3; they obtained values for the energy of the $(0/+)$ occupancy level and of the deep $(0/+)$ level of the three species. The far-IR results demonstrate that the bistable series (*D*, *E*, *F'*), *F* and *G* belong to different TD species (which also are different from the species giving rise to the series *H*, *I*, and *J*), and it was also shown in Ref. 6 that the “earliest” (*D*, *E*, *F'*) series most probably belong to the same TD species. It is therefore straightforward to assign (*D*, *E*, *F'*), *F*, and *G* to TD1, TD2, and TD3, respectively. The latter assumption has been substantiated by Clauws and Vennik in two ways.⁷ First, the Fermi-level dependence of the bistability in the three cases shown in Fig. 1 was demonstrated to be in agreement with the position of the three $(0/+)$ occupancy levels obtained by Litvinov, Palchik, and Urenev. Second, the parameters of the activated time constant of the shallow-to-deep configurational transformation were determined for (*D*, *E*, *F'*) and *F*; these were shown to practically coincide with the parameters determined in Refs. 4 and 5 for TD1 and TD2, respectively.

The consequent assignment of the far-IR series to the sequence of TD species numbered 1 to 6 is summarized in the first two columns of Table II. For TD4 to TD6 the

TABLE II. Assignment of spectra of neutral thermal donors in germanium to numbered members in the hierarchy, from the correlation of electrical, far-IR, and EPR data. The assignment of the electron paramagnetic resonances is also illustrated in Fig. 2.

	Far-IR	EPR
TD1	<i>D</i> , <i>E</i> , <i>F'</i>	
TD2	<i>F</i>	C_{2v} (spectrum 1)
TD3	<i>G</i>	C_{3v} (spectrum 2,3)
TD4	<i>H</i>	C_{3v} (spectrum 2,3)
TD5	<i>I</i>	C_{2v} (new spectrum)
TD6	<i>J</i>	

assignment was made taking account of the sequential appearance of *H*, *I*, and *J* and of the observation that at least *H* and *I* belong to different TD species, regarding their different relative contribution at different stages of TD formation. In the following section the correlation of TD species observed in far-IR and EPR results will be investigated.

B. EPR results

The investigation of EPR spectrum 1 by Callens *et al.*⁸ and by Bekman *et al.*⁹ was made using samples corresponding with the case of Fig. 1(b). Bekman *et al.* observed 100% bistability of spectrum 1, upon cooling with illumination compared to cooling in the dark; this allowed them to assign spectrum 1 to donor series *F*. In those samples, small traces of EPR spectra 2 and 3 were also observed, which remained unchanged; it was therefore suggested in Ref. 9 that EPR spectra 2 and 3 possibly correspond to the far-IR series *G* and *H*, although the evidence was considered insufficient.

For the present investigation the samples were either slowly cooled in the dark or quenched by insertion of the sample holder in the cold helium exchange gas of the cryostat. For samples of the type corresponding to Fig. 1(b), bistability of spectrum 1 was observed, confirming the assignment of Bekman *et al.*.

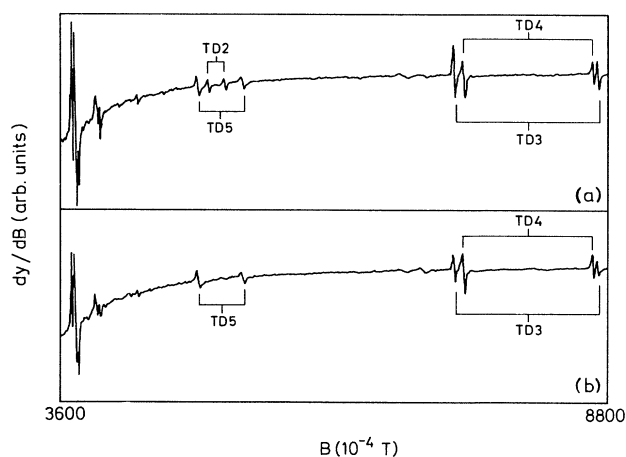


FIG. 2. Observation of bistable behavior in the EPR spectrum of neutral thermal donors in germanium; the sample data are the same as for the far-IR reference spectrum of Fig. 1(c), $T=4.5$ K. (a) Sample quenched to 70 K within a few seconds. (b) Sample slowly cooled in the dark (3 K/min). The two spectra have been drawn on the same scale.

The results for the case corresponding to Fig. 1(c) is shown in Fig. 2, for the magnetic field parallel to the $\langle 111 \rangle$ direction (in this orientation, spectra with different symmetry appear well separated; the angular dependence of TD spectra with C_{2v} and C_{3v} symmetry has been given in Ref. 8). Four different spectra are observed, the main resonances of which have been labeled TD2 to TD5 for reasons that will be explained later (the lines in the low-field range of Fig. 2 are due to other resonances from the same spectra, which are more difficult to separate when several TD species are simultaneously present).

In the quenched sample the spectrum contains resonances observed previously by Callens *et al.*,⁸ together with new lines. The two doublets labeled TD2 and TD5 in Fig. 2 are due to centers with C_{2v} symmetry. The inner doublet (labeled TD2) belongs to spectrum 1, which was discussed in detail in Refs. 8 and 9. The outer doublet (labeled TD5) consists of previously unobserved lines; it belongs to a new spectrum with the same angular variation as spectrum 1 (TD2), but with a different splitting of the C_{2v} branches. The resonances in the high-field part of the spectrum, labeled TD3 and TD4, are due to centers with trigonal symmetry (C_{3v}), which were already described by Callens *et al.*⁸ [Callens *et al.* designated the latter resonances as spectrum 2 and spectrum 3, spectrum 2 corresponding to the two lines at lower field and spectrum 3 with those at higher field; the following results demonstrate that fact the two outer lines belong to the same center (TD3) and the two inner lines belong to another center (TD4), both with trigonal symmetry.]

In the slowly cooled sample the lines of spectrum 1 (TD2) are missing, while the new C_{2v} spectrum (TD5) remains unchanged. As to the C_{3v} resonances, the two outer lines (TD3) are reduced to 50% of their original amplitude, while the inner two lines (TD4) remain unchanged.

The result in Fig. 2 is interpreted as follows: the spectrum contains contributions of four distinct centers, two with a C_{2v} pattern and two with a C_{3v} pattern. Centers with the same symmetry have comparable g factors; the splitting of the branches is different, however, allowing them to be separated. The g factors and the splittings that characterize the spectra for $B \parallel \langle 111 \rangle$ have been summarized in Table III.

The correlation of the EPR spectra in Fig. 2 with the far-IR spectra in Fig. 1(c) is straightforward, if one takes into account the bistability and the relative strength of the components. The correspondence of spectrum 1

(TD2) with donor series F made by Bekman *et al.* is again confirmed, since it is the only species with 100% bistability and since in both kinds of spectra the relative strength is similar. The outer C_{3v} doublet (TD3) obviously displays the same behavior as donor series G : in both cases the bistability amounts to about 50% and the components are the strongest in the quenched samples.

The inner C_{3v} doublet (TD4) and the new outer C_{2v} doublet (TD5), which remain unchanged, must be correlated with the donor series H and I , the importance of J being probably too small to yield a distinct signature in the EPR spectra. Considering the relative strength of the spectra, the most obvious assignment is the following: the C_{3v} spectrum (TD4) to series H and the C_{2v} spectrum (TD5) to series I .

The correspondences of the far-IR and EPR spectra have also been summarized in Table II, from which the assignment of the EPR spectra to TD2–TD5 follows immediately. This justifies the use of the corresponding resonance labels in Fig. 2 and Table III.

IV. SINGLY IONIZED THERMAL DONORS

The singly ionized state TD^+ can be observed in far-IR spectroscopy by raising the temperature above about 20 K, where the centers become thermally ionized; lists of series labels and line positions have been published by Clauws and Vennik.^{3,6} Thermal ionization, with a corresponding increase of the sample conductivity, is, however, unfavorable for EPR experiments. As an alternative the samples may be compensated, which was accomplished in the present case by diffusing copper into the oxygen-doped germanium; this was followed by a thermal donor formation anneal until partial compensation was established (substitutional copper is a triple acceptor in germanium¹⁰).

A. Far-IR results

Following quenching, the series F^0 , G^0 , and H^0 are observed. This absorption disappears after slow cooling, and the lines of F^+ , G^+ , and H^+ , appear instead, as shown in the far-IR reference spectrum of Fig. 3, where again the $1s \rightarrow 2p_0$ range has been reproduced (the latter lines coincide with the range of the $1s \rightarrow np_{\pm}$ transitions of the neutral donors; this range becomes optically transparent when the concentration of neutral donors is small). Spectra recorded under continuous band-gap pumping, which practically eliminates the compensation and allows one to “count” the full amount of shallow donors, reveals that the different result of slow cooling and quenching is mainly a consequence of the bistability of TD2 (series F). The smaller total density of shallow donors in the slowly cooled sample results in a higher compensation degree, sufficient to convert most centers into the TD^+ state.

B. EPR results

The spectrum of the quenched sample is quite complicated and is dominated by resonances from TD2, with

TABLE III. g factors and doublet splittings characterizing the electron paramagnetic resonances of neutral thermal donors in germanium for $B \parallel \langle 111 \rangle$ (see Fig. 2 for the assignments): $g_{\langle 111 \rangle}$, g value from midpoint of the doublet; $\Delta_{\langle 111 \rangle}$, splitting of the doublet at 9.47 GHz.

	$g_{\langle 111 \rangle}$	$\Delta_{\langle 111 \rangle}$ (T)
TD2	1.329 ± 0.005	0.0154
TD3	0.846 ± 0.005	0.1357
TD4	0.843 ± 0.005	0.1220
TD5	1.320 ± 0.005	0.0427

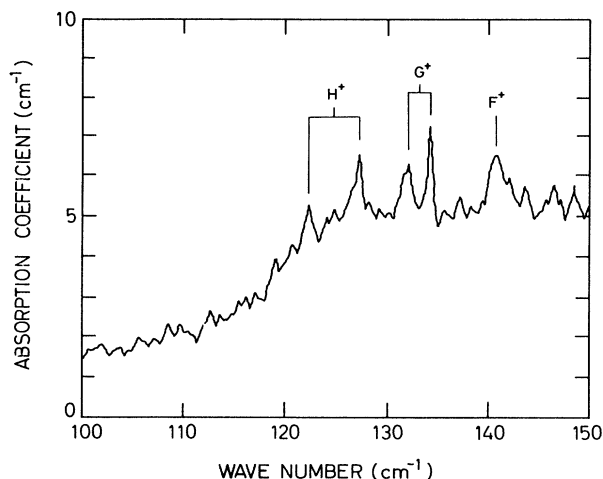


FIG. 3. Far-IR spectrum of thermal donors in an oxygen-doped germanium sample that was compensated by copper diffusion; TD formation at 360°C, 15 min; $n(300\text{ K}) = 1.7 \times 10^{15}\text{ cm}^{-3}$; $1s \rightarrow 2p_0$ transitions; measurement temperature, $T \approx 7\text{ K}$. The sample was slowly cooled in the dark (3 K/min).

contributions of TD3 and TD4 in agreement with the far-IR reference. After slowly cooling, most lines disappear and a simple spectrum with single lines remains. The angular variation of the latter spectrum is displayed in Fig. 4. The pattern is typical of centers with C_{3v} symmetry in the diamond lattice and the data can be fitted with a simple g tensor, assuming $S = \frac{1}{2}$. The principal g values are

$$g_{\parallel} = 0.854 \pm 0.005, \quad g_{\perp} = 1.921 \pm 0.005,$$

with g_{\parallel} corresponding to the $\langle 111 \rangle$ direction. Compar-

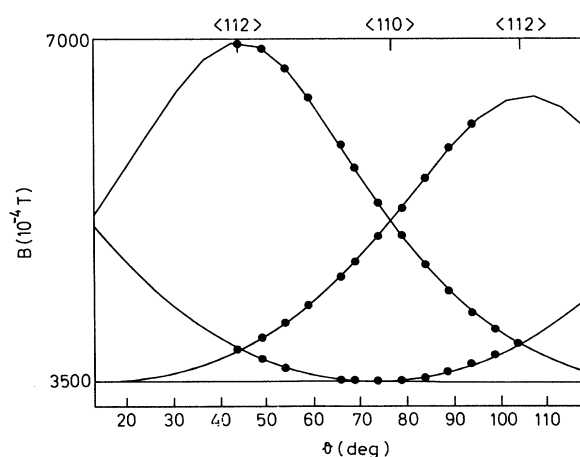


FIG. 4. Angular dependence of the EPR spectrum of thermal donors in the same oxygen-doped and compensated sample as in Fig. 3. The sample was slowly cooled in the dark (3 K/min). $T = 4.1\text{ K}$, microwave power 5 mW, the rotation axis shows a small offset from the $\langle 111 \rangle$ direction. The solid lines represent a computer fitting with an axial g tensor with axis $\parallel \langle 111 \rangle$.

ison with the far-IR reference indicates that the spectrum must be due to singly ionized thermal donors.

V. DISCUSSION

The correspondence of the far-IR and EPR spectra of the neutral thermal donors, as summarized in Table II, seems to be well established from the preceding. The assignment to species in the TD hierarchy, i.e., to TD2-TD5, relies, however, on the correct assignment of (D, E, F') to TD1. As explained earlier, the series (D, E, F') are the "earliest" that have been detected in "oxygen-only" samples with small or moderate oxygen doping, and they always appear together with similar relative amplitude, irrespective whether the concentration is 10^{10} or 10^{14} TD/cm^3 .⁶ This suggests that the series are intimately related and that they probably belong to the same TD species, which also would be the first member in the hierarchy. The correspondence of (D, E, F') to TD1 characterized by Litvinov, Palchik, and Urenev^{4,5} is further substantiated by (i) the maximum concentration of the species of about $10^{14}\text{ defects/cm}^3$, (ii) the straightforward explanation of bistability from the Fermi-level position with respect to the TD1 $(0/+ +)$ occupancy level, and (iii) the identical parameters of the activated time constant describing the annealing of the metastable state.⁷ Attempts to observe EPR spectra in samples containing TD1 have so far been unsuccessful, probably because the TD concentration is below the detection limit in samples of the dimensions presently used.

The EPR spectrum of the ionized TD's with trigonal symmetry (Fig. 4) is considered to correspond primarily to TD3^+ , since G^+ is the strongest series in the far-IR reference spectrum. As will be discussed below, the unsplit C_{3v} pattern in Fig. 4 is essentially determined by the g factors of the conduction-band valleys, and one may therefore predict that resonances from TD4^+ (H^+ in the far-IR reference) will practically coincide with those from TD3^+ , provided the symmetry is the same as in the neutral charge state. We may therefore conclude that the observed spectrum very probably consists of a superposition of TD3^+ and TD4^+ . Resonances from TD2^+ , expected to display a C_{2v} pattern, are probably too weak to be detected in the slowly cooled sample.

Regarding the high density of copper impurities in the compensated sample, we should also consider the possibility that copper may be involved in the center responsible for the EPR spectrum of Fig. 4. Copper is known to form a number of complexes with other impurities (see, e.g., Haller and co-workers^{11,12}); moreover, Fuller noticed an influence of copper on the TD formation rate in germanium.¹³ It follows, however, from our earlier investigations³ that, among the far-IR series discovered so far, only A^+ , B^+ , and C^+ show a possible correlation with copper; the series D to J are observed regardless of copper doping. In the far-IR reference spectrum of Fig. 3, only lines from F^+ , G^+ , and H^+ are present, so that copper involvement in the EPR spectrum of Fig. 4 seems rather unlikely. For a more systematic investigation of singly ionized TD centers, the use of oxygen-doped germanium crystals compensated by various acceptors

would be preferable.

The g factors of the spectra can be straightforwardly derived from the g factors of the conduction-band valleys of germanium, as expected for shallow donor centers. The ground-state wave function of an effective-mass donor in germanium can be described as¹⁴

$$\Psi_{1s} = \sum_{j=1}^4 \alpha_j \Phi_{1s}^{(j)}, \quad (1)$$

with the $\Phi_{1s}^{(j)}$ representing single-valley $1s$ wave functions; $j=1,2,3$, and 4 indicates the corresponding conduction-band valleys with axes in the $[111]$, $[\bar{1}\bar{1}1]$, $[1\bar{1}\bar{1}]$, and $[\bar{1}1\bar{1}]$ directions, respectively. The tensor $\tilde{g}^{(j)}$ of each valley is characterized by g_{\parallel} and g_{\perp} ; ^{15–20} the g tensor of the state described by (1) is then given by ¹⁵

$$\tilde{g} = \sum_j (\alpha_j)^2 \tilde{g}^{(j)}. \quad (2)$$

Donors with T_d symmetry have equal α_j and a scalar $g = g_0 = (g_{\parallel} + 2g_{\perp})/3$; in this case, values for g_{\parallel} and g_{\perp} can be obtained from experiments under uniaxial stress. Experimental and theoretical g values for shallow donors in germanium are summarized in Table IV.

Centers with C_{2v} symmetry in the diamond lattice, with the twofold axis along the $\langle 100 \rangle$ directions and with $\{110\}$ mirror planes, give rise to an EPR spectrum with the typical pattern of spectrum 1 (see Fig. 1 in the paper of Callens *et al.*;⁸ the g tensor that was obtained represents an average, neglecting the doublet splitting of the resonances). If we take the center with the twofold axis $||[001]$ and mirror planes $\sigma_v = (\bar{1}10)$, $\sigma'_v = (110)$ as the standard orientation among the six equivalent ones, the experimental g tensor of spectrum 1 (TD2⁰), with $g[001] = 1.575$, $g[\bar{1}10] = 1.917$, $g[110] = 1.190$, is in agreement with an effective-mass donor state constructed from two valleys:

$$\Psi_{1s} = (1/\sqrt{2})(\Phi_{1s}^{(1)} \pm \Phi_{1s}^{(2)}), \quad (3)$$

with valleys $j=1$ and 2 having their axis in the σ_v mirror plane. The single-valley g values reproducing the experimental data for TD2⁰, with the ground state given by (3), have been included in Table IV; the excellent agreement with the data for other shallow donors is obvious. The

same picture as for TD2⁰ applies to TD5⁰, which has a similar angular variation and almost identical “average” g factors.

The ground-state composition given by (3) may be brought about by a local C_{2v} strain introduced by the defect; a strain with this symmetry is described by a strain tensor $\epsilon_{xx} = \epsilon_{yy}, \epsilon_{zz}, \epsilon_{xy}$. According to the deformation-potential theory,²¹ among the components above only ϵ_{xy} is effective in inducing a relative shift of the conduction-band valleys in germanium. With $\epsilon_{xy} < 0$, the valleys $j=1,2$ are lowered with respect to the valleys $j=3,4$; a similar strain is compressive in the σ_v plane and tensile or less compressive in the σ'_v plane; the effect on the valleys is similar as for a uniaxial stress along $[110]$.^{15,22} Ham²³ states that the energy change of an effective-mass donor state is obtained by averaging over the strain distribution weighted with the probability distribution of the electronic wave function; for a local strain, the effect is accordingly the largest for the $1s$ states. It is easily shown that the $1s$ states belonging to the valleys $j=1,2$ become decoupled from the $1s$ states belonging to the valleys $j=3,4$ when the effect of the local C_{2v} strain exceeds the valley-orbit energies. The ground-state composition of TD2⁰ and TD5⁰ given by (3), which is necessary to explain the experimental g factors, is accordingly in agreement with a local C_{2v} strain that is compressive in the σ_v ($\bar{1}10$) plane of the defect. It may be remembered that the ground state of the TD's in silicon is equally constructed from only two valleys, which are directed along the twofold axis of the defect;^{24,25} the strong ϵ_{zz} component of the local strain explaining this valley selection has, however, no effect on the valleys in germanium.

The angular variation of the EPR spectrum of TD3⁰ and TD4⁰, and of the (TD3⁺, TD4⁺) spectrum in Fig. 4, is typical of axial centers with axes in the $\langle 111 \rangle$ directions. The “average” g factors g_{\parallel} and g_{\perp} of TD3⁰ and TD4⁰, as well as the values of (TD3⁺, TD4⁺) given in Sec. IV B are in excellent agreement with the g factors of the conduction-band valleys (Table IV). Taking the defect with the axis $||[111]$ as the standard orientation, this means that the $1s$ ground state of the center belongs to the valley $j=1$ only. An obvious mechanism for a similar valley selection is a local C_{3v} strain, which is compressive in the direction of the $[111]$ axis; this kind of strain is known to lower the valley $j=1$ with respect to the other three valleys.¹⁵ Decoupling of the $1s$ state belonging to $j=1$ from the states belonging to $j=2,3,4$ is again obtained when the strain is sufficiently strong to overcome valley-orbit effects.

An EPR spectrum with a similar angular variation and almost the same g factors as the center in Fig. 4, was found earlier for the Li-O donor in germanium by Haller and Falicov^{17,18} (Table IV); the spectrum was assigned to single-valley, $\langle 111 \rangle$ oriented defects. The far-IR spectrum of Li-O, however, was interpreted in terms of the tunneling of the defect among the four equivalent orientations in real space. The single-valley nature of the EPR spectrum was explained by the tunneling frequency being much smaller than the EPR frequency, so that the defect appears located in one real-space orientation during a res-

TABLE IV. One-valley g values of shallow donors in germanium.

	g_0	g_{\parallel}	g_{\perp}	Reference
P	1.563	0.83	1.93	15
As	1.570	0.87	1.92	15
Sb	1.561	0.842	1.917	16
Bi	1.567			15
Li-O		0.859	1.904	17,18
Theory		0.98	2.07	19
Theory		0.87	2.08	20
TD2 ⁰		0.849	1.917	8
TD3 ⁰ , TD4 ⁰		0.85	1.90	8
TD3 ⁺ , TD4 ⁺		0.854	1.921	This work

onance event.¹¹ Both Li-O and TD3⁺ (and TD4⁺) are one-electron donors described by $S = \frac{1}{2}$; the almost identical EPR spectrum merely indicates that the valley composition of the ground state is very similar in both cases (neglecting effects from tunneling). The selection of one valley may for both defects be due to a compression of the neighboring lattice, in the direction of the [111] axis of the defect; the $\langle 111 \rangle$ strain was also suggested by Ham²³ for the Li-O and the O-H defect in germanium.

Callens *et al.* suggested that the splitting of the C_{2v} pattern of TD2⁰ (spectrum 1 in Ref. 8) and the deviation of the branches from the angular variation expected for $S = \frac{1}{2}$ were to be explained as due to centers with $S = 1$. Later, Bekman *et al.*⁹ obtained a complete fit of the angular variation, assuming $S = 1$ and including an unusual B^2S^2 term in the spin Hamiltonian. The present observations reveal that a similar situation is typical of all four of the neutral TD species, which display splitted C_{2v} or C_{3v} patterns. This is in obvious contrast to the simple $S = \frac{1}{2}$ angular dependence of (TD3⁺, TD4⁺) in Fig. 4, which demonstrates that the phenomenon is typical of the two-electron states of the neutral donors; this makes the assignment of the complicated patterns to $S = 1$ centers even more acceptable. It remains, however, to be examined in detail whether the spin Hamiltonian put forward by Bekman *et al.* is able to serve as a common model for all four donor species. The question also remains as to why neutral thermal donors in germanium give rise to a state with parallel spins, which is considerably populated at very low temperature. In heliumlike atoms, the 1s ground state has $S = 0$; neutral double donors in multiple-valley semiconductors will, however, have both spin-singlet and spin-triplet states in the 1s multiplet, the number depending on the splitting according to the donor symmetry. The EPR results seem to indicate that for TD's in germanium the situation is favorable for a low-lying 1s spin-triplet state. A similar suggestion was made earlier by Clauws and Vennik⁶ with respect to the occurrence of the TD series (D, E, F') in the far-IR spectrum.

The different symmetry of the spectra and the different splittings represent a fortunate situation allowing the separation of different TD species in germanium by EPR, offering interesting perspectives for future investigations.

As to the TD⁺ spectra, one may expect that resonances from donor species displaying patterns of the same symmetry will not be resolved and that only a shift of the average position may be detected, similarly to the case of Si-NL8 (TD⁺) species.^{26,27}

A final remark may be made concerning the symmetry of the spectra in relation to the microscopic structure of the defects. To the extent that the EPR spectrum reflects the true site symmetry of the defect, the results indicate that in germanium the symmetry of thermal donors changes from C_{2v} to C_{3v} and back as the oxygen agglomeration proceeds, in contrast to silicon where the C_{2v} symmetry is conserved (see, e.g., Refs. 26 and 27). Regarding the many similarities of thermal donor properties in the two semiconductors, the basic model cannot be too different, however, especially the composition of the core, which is considered to be determinative for the double donor character. From their recent electron-nuclear double resonance (ENDOR) results, Michel, Niklas, and Spaeth²⁷ conclude that for at least five TD⁺ species in silicon, the donor core contains four oxygen atoms on the (110) mirror planes. If the donor core would be considered to have a similar composition in germanium, then the present result suggests that at least some rearrangement of the core should be envisaged, possibly accompanied by the agglomeration of interstitial oxygen atoms in different directions. With our present knowledge precise models are too speculative and more evidence must be awaited, such as the symmetry of the TD1 spectrum from EPR or information on atomic positions from ENDOR. The larger extension of the electronic wave functions of TD's in germanium as compared to silicon is, however, unfavorable to the latter technique. With the present samples, ENDOR may reveal positions of germanium neighbors or incorporation of impurities other than oxygen. For the observation of oxygen ENDOR shells, doping with ¹⁷O in the melt or by diffusion will be necessary.

ACKNOWLEDGMENTS

This work is part of a project sponsored by Interuniversitair Instituut voor Kernwetenschappen, Belgium. One of us (F.C.) acknowledges financial support by the National Fund for Scientific Research, Belgium.

¹P. Clauws and J. Vennik, Phys. Rev. B **30**, 4837 (1984).

²P. Clauws, E. Simoen, and J. Vennik, in *Proceedings of the ICDS-13, Coronado, 1984*, edited by L. C. Kimerling and J. M. Parsey, Jr. (American Institute of Mining, Metallurgical and Petroleum Engineers, Pittsburgh, 1985), p. 911.

³P. Clauws and J. Vennik, in *Proceedings of the ICDS-14, Paris, 1986* [Mater. Sci. Forum **10-12**, 941 (1986)].

⁴V. V. Litvinov, G. V. Palchik, and V. I. Urenev, Fiz. Tekh. Poluprovodn. **19**, 1366 (1985) [Sov. Phys.—Semicond. **19**, 841 (1985)].

⁵V. V. Litvinov, G. V. Palchik, and V. I. Urenev, Phys. Status Solidi A **108**, 311 (1988).

⁶P. Clauws and J. Vennik, in *Proceedings of the ICDS-15, Bu-*

dapest, 1988 [Mater. Sci. Forum **38-41**, 473 (1989)].

⁷P. Clauws and J. Vennik, in *Proceedings of the ICSIS-IV, London, 1990* [Mater. Sci. Forum **65-66**, 339 (1990)].

⁸F. Callens, P. Clauws, P. Matthys, E. Boesman, and J. Vennik, Phys. Rev. B **39**, 11 175 (1989).

⁹H.H.P.T. Bekman, T. Gregorkiewicz, I.F.A. Hidayat, C.A.J. Ammerlaan, and P. Clauws, Phys. Rev. B **42**, 9802 (1990).

¹⁰H. H. Woodbury and W. W. Tyler, Phys. Rev. **105**, 84 (1957).

¹¹E. E. Haller, W. L. Hansen, and F. S. Goulding, Adv. Phys. **30**, 93 (1981).

¹²E. E. Haller, in *Festkörperprobleme (Advances in Solid State Physics)*, edited by P. Grosse (Vieweg, Braunschweig, 1986), Vol. 26, p. 203.

- ¹³C. S. Fuller, *J. Phys. Chem. Solids* **19**, 18 (1961).
¹⁴W. Kohn, in *Solid State Physics*, edited by F. Seitz, D. Turnbull, and H. Ehrenreich (Academic, New York, 1957), Vol. 5, p. 257.
¹⁵D. K. Wilson, *Phys. Rev.* **134**, A265 (1963).
¹⁶R. E. Pontinen and T. M. Sanders, Jr., *Phys. Rev.* **152**, 850 (1966).
¹⁷E. E. Haller and F. L. Falicov, *Phys. Rev. Lett.* **41**, 1192 (1978).
¹⁸E. E. Haller and F. L. Falicov, *Inst. Phys. Conf. Ser.* **43**, 1039 (1979).
¹⁹L. M. Roth, *Phys. Rev.* **118**, 1534 (1960).
²⁰L. Liu, *Phys. Rev.* **126**, 1317 (1962).
²¹C. Herring and E. Vogt, *Phys. Rev.* **134**, A265 (1964).
²²P. J. Price, *Phys. Rev.* **104**, 1223 (1956).
²³F. S. Ham, *Phys. Rev. B* **38**, 5474 (1988).
²⁴M. Stavola and K. M. Lee, in *Oxygen, Carbon, Hydrogen and Nitrogen in Crystalline Silicon*, edited by J. C. Mikkelsen and J. W. Corbett, MRS Symposia Proceedings No. 59 (Materials Research Society, Pittsburgh, 1986), p. 95.
²⁵P. Wagner, H. Gottschalk, J. M. Trombetta, and G. D. Watkins, *J. Appl. Phys.* **61**, 346 (1987).
²⁶S. H. Muller, M. Sprenger, E. G. Sieverts, and C.A.J. Ammerlaan, *Solid State Commun.* **25**, 987 (1978).
²⁷J. Michel, J. R. Niklas, and J. M. Spaeth, *Phys. Rev. B* **40**, 1732 (1989).